

Orbital Parameters and Spectroscopy of the transient X-ray Pulsar 4U 0115+63

Sebastian Müller*, Maria Obst, Ingo Kreykenbohm, Felix Fürst, Matthias Kühnel,
Jörn Wilms

Dr. Karl Remeis-Observatory & ECAP, University Erlangen-Nuremberg, Bamberg, Germany
E-mail: Sebastian.Mueller@sternwarte.uni-erlangen.de

Dmitry Klochkov, Rüdiger Staubert, Andrea Santangelo

Institut für Astronomie und Astrophysik, Tübingen, Germany

Katja Pottschmidt

*CRESST and NASA Goddard Space Flight Center, Greenbelt, MD, USA / Center for Space
Science and Technology, UMBC, Baltimore, MD, USA*

Slawomir Suchy, Richard E. Rothschild

Center for Astrophysics & Space Sciences, UCSD, La Jolla, CA, USA

Isabel Caballero

*CEA Saclay, DSM/IRFU/Sap – UMR AIM (7158) CNRS/CEA/Université Paris 7, Diderot, Gif
sur Yvette, France*

Peter Kretschmar

ISOC, European Space Astronomy Centre, ESA, Madrid, Spain

Gabriele Schönherr

Astrophysikalisches Institut Potsdam, Germany

We report on an outburst of the high mass X-ray binary 4U 0115+63 with a pulse period of 3.6 s in spring 2008 as observed with *INTEGRAL* and *RXTE*. By analyzing the lightcurves we derive an updated orbital- and pulse period ephemeris of the neutron star. We also study the pulse profile variations as a function of time and energy as well as the variability of the spectral parameters. We find clear evidence for at least three cyclotron line features. In agreement with previous observations of 4U 0115+63, we detect an anti-correlation between the luminosity and the fundamental cyclotron line energy.

8th INTEGRAL Workshop “The Restless Gamma-ray Universe”

September 27-30 2010

Dublin Castle, Dublin, Ireland

*Speaker.

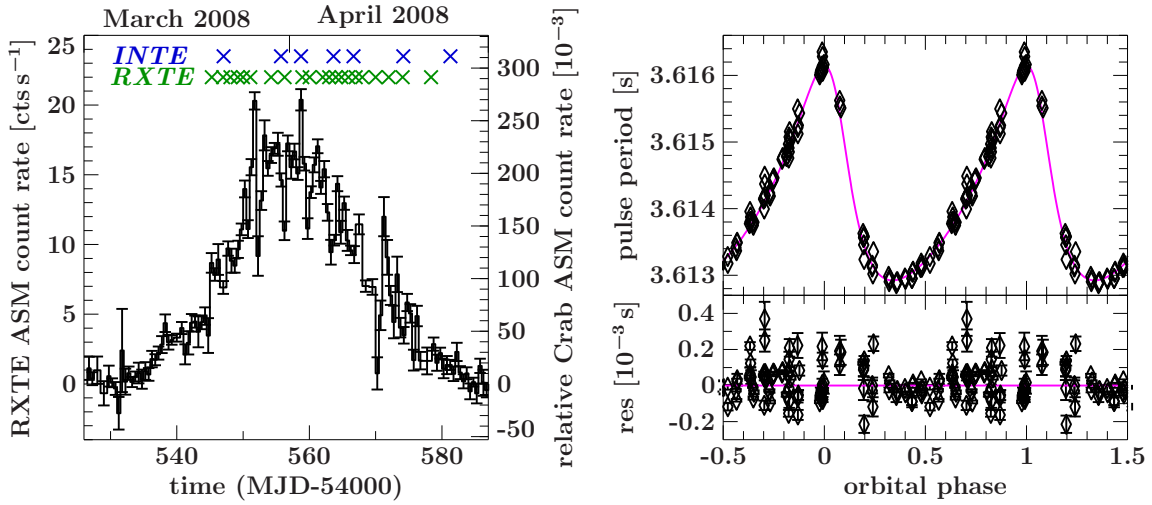


Figure 1: Left: *RXTE* ASM lightcurve of the outburst in spring 2008 with a binning of 0.5 days together with the observation times of *RXTE* (green) and *INTEGRAL* (blue). Right: Doppler shifted pulse periods of 4U 0115+63 versus the orbital phase together with the best fit ($\phi = 0$ where pulse period is at maximum).

1. Introduction

4U 0115+63 is a transient X-ray pulsar with a Be star optical companion. Unlike ordinary B stars, Be stars host a circumstellar disc, resulting from fast rotation, magnetic loops, or non-radial pulsations. Due to the highly eccentric orbit of the system, material originating from a Be star's disc can be accreted onto the neutron star during the periastron passage. One of the main processes leading to the observed hard X-ray emission is the Comptonisation of seed photons, e.g., from blackbody radiation of a hot spot on the neutron star surface, in the hot plasma of the accretion column above the magnetic poles.

On the surface of neutron stars magnetic fields of the order of 10^{12} G can occur. As a consequence, the X-ray spectra of pulsars may contain cyclotron resonance scattering features (CRSF) at a fundamental line energy of

$$E_c[\text{keV}] = 11.6 \times \left(\frac{B[10^{12} \text{G}]}{1 + z_g} \right) \quad (1.1)$$

as well as at the associated harmonic energies, where z_g is the gravitational redshift. So far CRSFs have been detected in about 20 X-ray pulsars.

4U 0115+63 is one of the pulsars for which CRSFs have been studied in great detail (see, e.g., [4, 5, 8, 9, 11, 13, 14]). In previous outbursts, CRSFs have been detected up to the fourth harmonic [11]. This high number of detected CRSFs in 4U 0115+63 makes this system an outstanding laboratory to study the physics of cyclotron lines in X-ray pulsars.

The overall lightcurve of the outburst we report on is shown in Fig. 1 (left). The event took place in spring 2008, with the peak intensity amounting up to ~ 280 mCrab. The outburst was observed in 21 individual *RXTE*- and 8 *INTEGRAL* pointings.

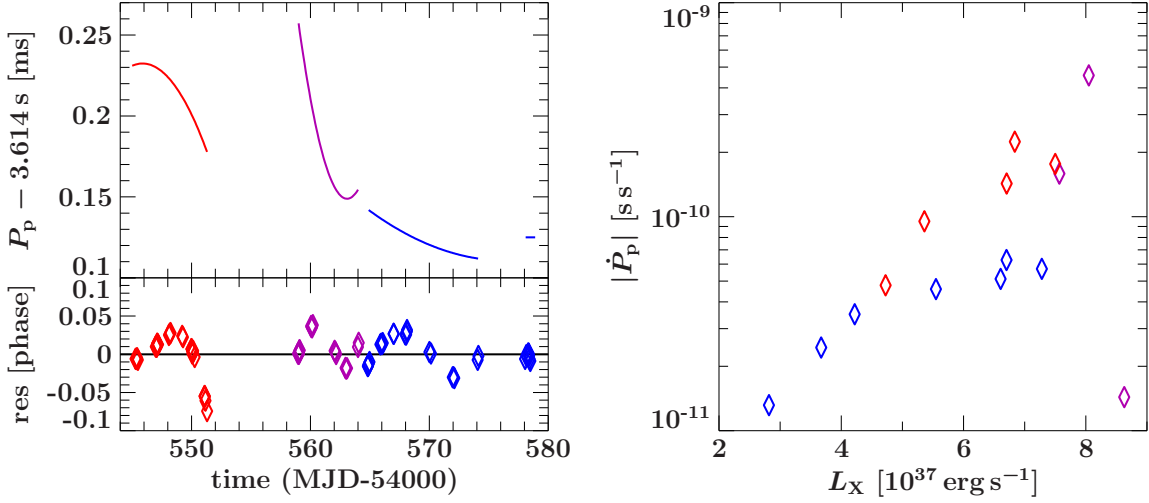


Figure 2: Left: Pulse period ephemeris based on the binary-corrected pulsar lightcurves derived by phase connection (top panel) and the phase shift between the measured pulse profiles and the pulse period ephemeris (bottom panel). Right: \dot{P} versus the luminosity. The colours red, purple, and blue correspond to the brightening phase, the outburst's maximum, and the dimming phase, respectively. Both figures are preliminary.

2. Orbital Ephemeris

Due to the orbital motion of the neutron star, its pulse period is Doppler shifted periodically (see Fig. 1, right). These shifted periods, calculated by epoch folding the PCA-lightcurves, can be used to refine the orbital ephemeris of the binary system. We used the orbital parameters from the literature [1] ($a_x \sin i = 140.13(8)$ lt-sec, $e = 0.3402(2)$ and $\omega = 47.66(9)^\circ$) except the epoch of periastron passage, T_0 , which we determined from the fit. Assuming that the orbital period P_{orb} remains constant, the difference between our T_0 and that from [1] has to be an integer times P_{orb} . This leads to $P_{\text{orb}} = 24.31617^{+0.00005}_{-0.00007}$ d. Recently, evidence for a non zero time derivation of the longitude of periastron $\dot{\omega}$ has been found [10]. The study of how this evolution affects our results is still work in progress.

3. Pulse Period Ephemeris

Using the new orbital ephemeris, we corrected the PCA-lightcurves for binary motion. The remaining variations in the pulse period P_p are due to transfer of angular momentum of the accreted matter onto the neutron star. By epoch folding these corrected lightcurves and performing phase connection (see, e.g., [12]), we calculated the pulse period ephemeris displayed in Fig. 2 (left). The respective parameters are summarized in Table 1, while the pulse period at a certain time t can be calculated as

$$P(t) = P_p(T_{0,p}) + \dot{P}_p(t - T_{0,p}) + \frac{1}{2}\ddot{P}_p(t - T_{0,p})^2. \quad (3.1)$$

As the first and the second time derivative of the pulse period, \dot{P}_p and \ddot{P}_p , are expected to change significantly during the outburst, we analyzed four different time intervals separately. As displayed in Fig. 2 (left), the evolution of the pulse period is not continuous over the outburst. Especially

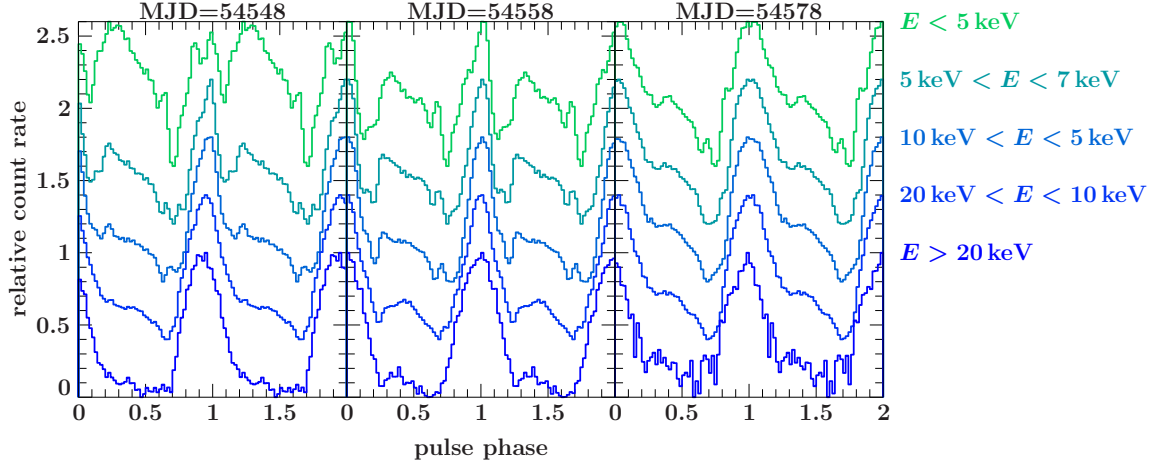


Figure 3: Pulse profiles of 4U 0115+63 for several energy bands and times.

the strong spin down-“jump” between the first and the second time interval is still not understood. Unfortunately there are only three data points available during this epoch. Because the times when the respective pulse profiles have been measured are too far away from the neighboring intervals, \dot{P}_p and \ddot{P}_p at these three points are expected to be different than during the intervals with a well constrained ephemeris. Therefore we had to omit these three data points from our analysis. Despite this enigmatic behaviour, the lower panel of Fig. 2 (left) shows that the phase shifts between the observed pulse profiles and the pulse period ephemeris (see Table 1) are small enough such that this pulse period ephemeris is suitable for phase resolved spectroscopy.

Fig. 2 (right) shows that the 3–50 keV luminosity and \dot{P}_p are correlated for the majority of data points. This is in agreement with the classical interpretation (see, e.g., [3], and references therein), where for higher luminosities a higher mass transfer rate and therefore a higher transfer of angular momentum is expected.

Table 1: Preliminary parameters of the pulse period ephemeris. The epochs are marked as follows: (i) $\text{MJD} < 54552.0$, (ii) $54557.0 < \text{MJD} < 54564.5$, (iii) $54564.5 < \text{MJD} < 54575.0$, and (iv) $\text{MJD} > 54575.0$

epoch	phase	$T_{0,p}$ (MJD)	$P_p(T_{0,p})$ [s]	\dot{P}_p [s s^{-1}]	\ddot{P}_p [s s^{-2}]
(i)	brightening	54550.055284	3.614200	-1.79×10^{-10}	-4.96×10^{-16}
(ii)	maximum	54558.948604	3.614260	-6.24×10^{-10}	$+1.75 \times 10^{-15}$
(iii)	dimming	54570.138089	3.614120	-3.43×10^{-11}	$+6.22 \times 10^{-17}$
(iv)	dimming	54578.350020	3.614125	± 0 (fix)	± 0 (fix)

4. Pulse Profile Variations

Pulse profiles for different energy bands and epochs are shown in Fig. 3. In agreement with previous work [1] the secondary peak is more prominent at lower energies, while at higher energies it disappears almost completely. These two peaks in the pulse profile are thought to originate from the two hot spots at the magnetic poles of the neutron star. An offset dipole field could explain

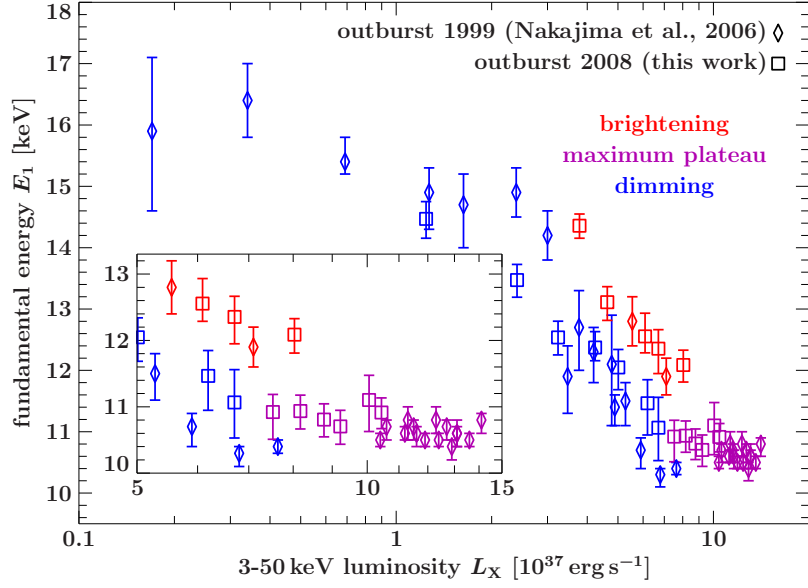


Figure 4: 3–50 keV luminosity versus fundamental cyclotron energies. The small box provides a close-up view for high luminosities. For $L_X \gtrsim 9 \times 10^{37} \text{ erg s}^{-1}$ the fundamental line energy stays nearly constant.

the different behaviour of the two pulse peaks, which has been observed in other transient X-ray sources as well (e.g., GRO J1008–57: [6], or 4U 1909+07: [2]).

5. Spectral fitting

We modelled PCA- and HEXTE data taken during the maximum of the outburst using the NPEX model (see., e.g. [7], and references therein), which can be written as

$$\text{NPEX}(E) = (A_1 E^{-\alpha_1} + A_2 E^{+\alpha_2}) \times \exp\left(-\frac{E}{kT}\right), \quad (5.1)$$

where $A_{1/2}$ are the normalization constants, $\alpha_{1/2}$ are the photon indices of the positive and negative powerlaws, and kT represents the cutoff energy. We included three cyclotron absorption features at $\sim 11, 22,$ and 33 keV using the model CYCLABS, which is given as

$$\text{CYCLABS}(E) = \exp\left(-\frac{\tau_n (W_n E / E_n)^2}{(E - E_n)^2 + W_n^2}\right), \quad (5.2)$$

where E_n is the n th resonance energy, W_n the corresponding width, and τ_n the optical depth. Furthermore we included a Gaussian iron emission feature at 6.4 keV and achieved an acceptable fit with $\chi_{\text{red}}^2 \approx 1.1$. Using these CRSF- and continuum parameters as a starting point and keeping $\alpha_2 = 2$, $E_2 = 2E_1$, and $W_2 = W_1$ fixed, we modelled all available spectra of the outburst. For all observations we obtained χ_{red}^2 between 1 and 2, but mostly less than 1.5. The photon index α_1 turned out to be constant within the uncertainties during the outburst and was therefore fixed to 1.2 to constrain the other parameters better. We determined values of 6.0 ± 0.2 keV for the cutoff energy kT in the beginning, and 4.6 ± 0.2 keV at the end of the outburst. While we found three cyclotron line features in all spectra until MJD=54568, after this time only the fundamental line

was detected. An anti-correlation between the fundamental cyclotron line energy and the 3–50 keV luminosity has been found for a previous outburst in 1999 [9]. As displayed in Fig. 4, this result is consistent with our new analysis. The hysteresis-like shape of the curve might be due to a change in the accretion geometry during the maximum of the outburst. This might be also the reason for the jump in the pulse period ephemeris of the neutron star detected during the maximum of the outburst.

6. Outlook

As forthcoming work we will check the consistency of the predicted changes in the periastron longitude [10] with our results. Furthermore we will analyze the phase resolved behavior of the spectral parameters, based on our updated pulse period ephemeris. For this purpose we will also include the *INTEGRAL* data into our spectral analysis.

7. Acknowledgments

This research was funded by the Bundesministerium für Wirtschaft und Technologie under Deutsches Zentrum für Luft- und Raumfahrt grant number 50 OR 0905.

References

- [1] L. Bildsten, D. Chakrabarty, J. Chiu, et al., *Observations of Accreting Pulsars*, *ApJS* **113**, 367 (1997).
- [2] F. Fürst, I. Kreykenbohm, S. Suchy, et al., *4U 1909+07: a well-hidden pearl*, *A&A*, in press (2010) [arXiv:astro-ph/1011.5052].
- [3] P. Ghosh and F. K. Lamb, *Accretion by rotating magnetic neutron stars. III - Accretion torques and period changes in pulsating X-ray sources*, *ApJ* **234**, 296–316 (1979).
- [4] W. Heindl, W. Coburn, D. E. Gruber, et al., *Discovery of a Third Harmonic Cyclotron Resonance Scattering Feature in the X-Ray Spectrum of 4U 0115+63*, *Astrophys. J., Lett.* **521**, L49–L53 (1999).
- [5] W. Heindl, W. Coburn, P. Kretschmar, et al., *Phase Resolved Spectroscopy of the Multiple Cyclotron Line Pulsar 4U 0115+63*, *APS Meeting Abstracts*, 17063 (2002).
- [6] M. Kühnel, et al., in preparation.
- [7] K. Makishima, T. Mihara, F. Nagase, and Y. Tanaka, *Cyclotron Resonance Effects in Two Binary X-Ray Pulsars and the Evolution of Neutron Star Magnetic Fields*, *ApJ* **525**, 978–994 (1999).
- [8] F. Nagase, T. Dotani, Y. Tanaka, et al., *Cyclotron line features in the spectrum of the transient X-ray pulsar X0115 + 63*, *Astrophys. J., Lett.* **375**, L49–L52 (1991).
- [9] M. Nakajima, T. Mihara, K. Makishima, and H. Niko, *A Further Study of the Luminosity-dependent Cyclotron Resonance Energies of the Binary X-Ray Pulsar 4U 0115+63 with the Rossi X-Ray Timing Explorer*, *ApJ* **646**, 1125–1138 (2006).
- [10] H. Raichur and B. Paul, *Apsidal motion in 4U0115+63 and orbital parameters of 2S1417-624 and V0332+53*, *MNRAS* **406**, 2663–2670 (2010).
- [11] A. Santangelo, A. Segreto, S. Giarrusso, et al., *A BEPPOSAX Study of the Pulsating Transient X0115+63: The First X-Ray Spectrum with Four Cyclotron Harmonic Features*, *Astrophys. J., Lett.* **523**, L85–L88 (1999).
- [12] R. Staubert, D. Klochkov, and J. Wilms, *Updating the orbital ephemeris of Hercules X-1; rate of decay and eccentricity of the orbit*, *A&A* **500**, 883–889 (2009).
- [13] W. A. Wheaton, J. P. Doty, F. A. Primini, et al., *An absorption feature in the spectrum of the pulsed hard X-ray flux from 4U0115 + 63*, *Nat* **282**, 240–243 (1979).
- [14] N. E. White, J. H. Swank, and S. S. Holt, *Accretion powered X-ray pulsars*, *ApJ* **270**, 711–734 (1983).